Scattering of 43-Mev α Particles by Nuclei*

J. L. YNTEMA, B. ZEIDMAN, AND B. J. RAZ†
Argonne National Laboratory, Lemont, Illinois
(Received August 5, 1959)

The differential scattering cross sections for the elastic scattering of 43-Mev α particles by Zn, Ag, Rh, and Au are obtained over the angular range from 12° to 55°. The absolute errors in the cross sections are estimated to be less than 2% over most of the angular range. The group structure in the inelastic spectrum observed with protons and deuterons is also observed with α particles. In the spectra of Ag, Rh, and Zn, one group near 2.7 Mev was observed. In Al, V, and Ni a number of groups were observed. In Au and Ta no groups could be resolved. Angular distributions were obtained for the 2.5-Mev group in Rh and Ag and the 2.8-Mev group in Zn. In the case of the 2.8-Mev group in Zn, the angular distribution shows a very marked diffraction pattern. The data were fitted with Butler's theoretical expression modified to eliminate the assumption that the scattering of 43-Mev α particles by nucleons is isotropic in the center-of-mass system. It is shown that this assumption can be easily eliminated in the formal treatment. A comparison with the angular distributions obtained for the 1.04-Mev 2^+ level in Zn with both 43-Mev α particles and 21.6-Mev deuterons indicates that $l=3$ is the most plausible assignment for the 2.8-Mev group.

I. INTRODUCTION

THE elastic scattering of alpha particles by nuclei has been measured at 18 Mev,[1,2] 22 Mev,[3] 29.5 Mev,[4] 40 Mev,[5–7] and 48 Mev.[8] The data have been analyzed in terms of an optical potential model,[9–12] and in terms of a sharp-cutoff theory developed by Blair.[13] In the analysis of the scattering of alpha particles by silver, Cheston and Glassgold[10] have found that if the data of Wall, Rees, and Ford[3] at 22 Mev are assumed to be free of systematic error, then the data of Igo, Wegner, and Eisberg at 40 Mev could be fitted with the same parameters for the optical potential only if a 25% correction were applied to the 40-Mev data. Furthermore it appeared that the oscillations in the theoretically predicted diffraction pattern at larger angles were more pronounced than the data seemed to indicate. However, at larger angles a relatively wide spacing of the experimental points and the larger angle subtended by the detector made a comparison difficult. In the present experiment the experimental data were obtained at 43 Mev, the angular range was extended to smaller angles, great care was taken to obtain absolute differential cross sections, and the angle subtended by the detector was substantially smaller than in the 40-Mev experiment.

In the process of obtaining the distributions of elastically scattered α particles, the inelastic spectra were also obtained. Sweetman and Wall[14] have obtained inelastic spectra near 30 Mev for a number of elements. They found a group structure similar to the ones obtained with protons[15] and deuterons[16] near 22 Mev. In some instances it was feasible to obtain angular distributions of inelastic groups.

II. EXPERIMENTAL PROCEDURE

The experiment was done with the 43-Mev alpha beam of the Argonne 60-in. cyclotron,[17] and the 60-in. scattering chamber.[18,19] The detector subtended an angle of 0.5 degree and consisted of two NaI(Tl) crystals which the particle traversed in series. The front (dE/dX) crystal was 0.003 in. thick and the back (E) crystal was 0.030 in. thick. To select pulses corresponding to the desired particle, the pulses from the dE/dX and E crystals were multiplied and the product pulse was used to gate the 100-channel analyzer.[20] The pulse height from the E crystal was transformed to an energy scale of scattered α particles by use of a system of absorber disks[21] and the range-energy relation for α particles in Al. In some instances it was desirable to obtain a better separation between the elastic peak and inelastically scattered α particles. This was done by inserting an absorber in front of the dE/dX crystal and making use of the curvature of the range-energy curve. Targets of Al, Ni, Zn, Rh, Ag, and Au were made of commercially available foils approximately 0.0001 in.

* Work performed under the auspices of the U. S. Atomic Energy Commission.
† Permanent Address: State University, College on Long Island, Oyster Bay, New York.
[1] Seidlitz, Bleuler, and Tendam, Phys. Rev. **110**, 682 (1958).
[2] Garlar, Bleuler, and Tendam, Phys. Rev. **112**, 1989 (1958).
[3] Wall, Rees, and Ford, Phys. Rev. **95**, 1212 (1954).
[4] H. E. Gove, Phys. Rev. **99**, 1353 (1955).
[5] Wegner, Eisberg, and Igo, Phys. Rev. **99**, 825 (1955).
[6] Eisberg, Igo, and Wegner, Phys. Rev. **99**, 1606 (1955).
[7] Igo, Wegner, and Eisberg, Phys. Rev. **101**, 1508 (1956).
[8] R. E. Ellis and L. Schechter, Phys. Rev. **101**, 636 (1956).
[9] G. Igo and R. M. Thaler, Phys. Rev. **106**, 126 (1957).
[10] W. B. Cheston and A. E. Glassgold, Phys. Rev. **106**, 1215 (1957).
[11] C. E. Porter, Phys. Rev. **112**, 1722 (1958).
[12] G. Igo, Phys. Rev. Letters **1**, 72 (1958).
[13] J. S. Blair, Phys. Rev. **95**, 1218 (1954).
[14] D. R. Sweetman and N. S. Wall, *Comptes Rendus à Congres International de Physique Nucléaire* (Dunod, Paris, 1959), p. 547.
[15] B. L. Cohen, Phys. Rev. **105**, 1549 (1957).
[16] J. L. Yntema and B. Zeidman, Phys. Rev. **114**, 815 (1959).
[17] W. Ramler and G. Parker, Argonne National Laboratory Report ANL-5907 (unpublished).
[18] J. L. Yntema, Phys. Rev. **113**, 261 (1959).
[19] J. L. Yntema, Argonne National Laboratory Report ANL-5890 (unpublished).
[20] J. P. McMahon (unpublished).
[21] O'Neill, Sundahl, and Ostrander, Nuclear Instr. and Methods **4**, 50 (1959).

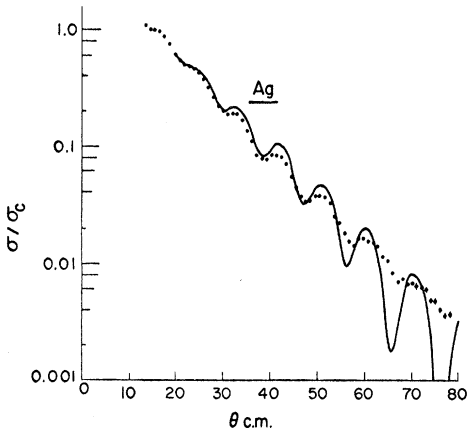

FIG. 1. The ratio of measured differential cross sections to Coulomb cross sections for Ag. The errors are smaller than the points, unless shown. The curve was taken from the paper by W. B. Cheston and A. E. Glassgold, Phys. Rev. **106**, 1216 (1957).

thick. The diameter of the foils was measured on a Zeiss comparator and the targets were weighed on a microbalance. Since there is some lack of uniformity in the original sheets, several targets of each element were used at one angle. The results obtained were consistent to within ±1%. Targets of Nb, Ta, and V were prepared from foils rolled at Argonne National Laboratory.[22] The thickness of these targets was not determined.

III. ELASTIC SCATTERING DATA

Elastic scattering data were obtained for Au, Ag, Rh, and Zn. The results have been tabulated both as absolute cross sections and as ratios to Rutherford cross sections and are available upon request.[23]

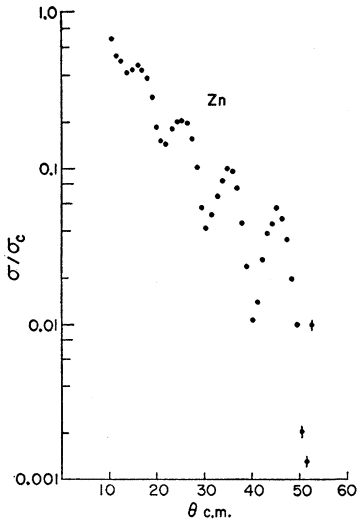

FIG. 2. The ratio of measured differential cross sections to Coulomb cross sections for Zn. The errors are smaller than the points, unless shown.

[22] We are indebted to Mr. Frank Karasek for the rolling of these materials.

[23] J. L. Yntema, Argonne National Laboratory Report ANL-5936 (unpublished).

The experimental results for Ag are shown in Fig. 1. The curve has been taken from the paper by Cheston and Glassgold.[10] The potential used was of the form $V(r)=Vf(r)+iWg(r)+V_c$ with

$$f(r)=g(r)=\{1+\exp[(r-R)/a]\}^{-1}.$$

The parameters of the curve shown were $V=-50$ Mev, $W=-20$ Mev, $R=7.5$ f, $a=0.6$ f. The experimental errors have been indicated whenever they were larger than the size of the points. The absolute error for all points at angles smaller than 50° is less than 2%. It is seen that at small angles the agreement between the experimental points and the curve is excellent, especially in view of the fact that the 22-Mev data have an assigned error of about 10%. The experimental diffraction pattern at large angles is less pronounced than the theoretical one. It might be possible that the levels below 1 Mev in Ag have contributed to a filling of the valleys. It is not believed that these levels were strongly excited in the present experiment. Corrections for multiple scattering and geometry[24] have been applied to the data and do not appear to have any effect on the depth of the valleys.

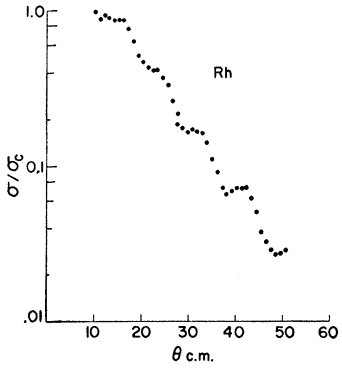

FIG. 3. The ratio of measured differential cross sections to Coulomb cross sections for Rh. The errors are smaller than the points.

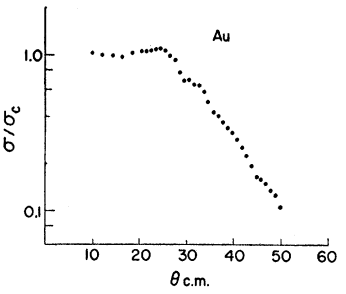

FIG. 4. The ratio of measured differential cross sections to Coulomb cross sections of Au. The errors are smaller than the points.

The results for Zn, Rh, and Au are shown in Figs. 2, 3, and 4, respectively. The low-lying levels in Au and Rh were not resolved. For Zn it was not possible to resolve the 1.04-Mev level at angles smaller than 28°. For all angles the experimental error is less than 2% when no error bars are shown. The curve for Au appears

[24] I. E. Dayton and G. Schrank, Phys. Rev. **101**, 1358 (1956).

to indicate a diffraction pattern although such a pattern did not appear to exist in the 40-Mev work. The 48-Mev data[8] show an oscillation comparable to the one in the present data.

The spectra for inelastic scattering of α particles at 30 Mev have been obtained by Sweetman and Wall[14] for a number of elements. The data obtained for Al show peaks at about 3.4, 5.7, and 8.0 Mev. For V, groups were obtained at 2.4, 4.1, and 7.5 Mev; for Ni at about 1.7, 4.8, 7.1, and 11 Mev; and for Rh at about 2.5 Mev. The energies refer to the excitation of the final nucleus. The spectra obtained at 30° for Al, V, Ni, and Zn are shown in Fig. 5. At this angle the low-energy groups are considerably more difficult to separate from the elastic peak than at larger angles

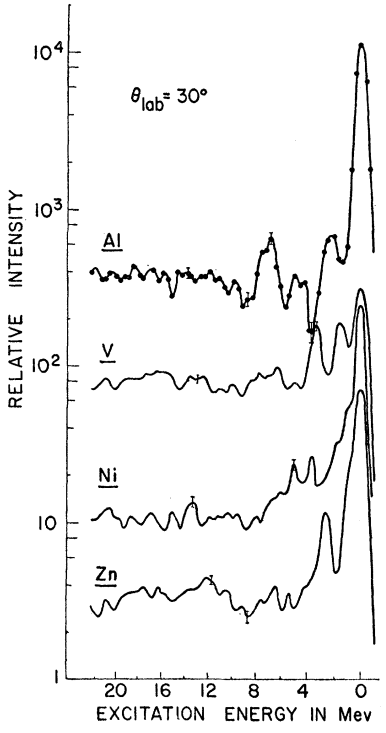

FIG. 5. The inelastic α-particle spectra from Al, V, Ni, and Zn. The abscissa is the excitation energy of the final nucleus. The points together with representative statistical errors are shown for Al. For V, Ni, and Zn the curve has been drawn through the experimental points.

because of the intensity of the latter. It is seen that there are peaks in Al at 2.5, 5.0, and 7.2 Mev; for V the peaks are at 1.8 and 3.2 Mev; for Ni at 1.8 Mev, 3.4 Mev, 5.0 Mev, and a statistically nonsignificant group at 13 Mev; for Zn at 2.8 Mev. The energies again refer to the excitation energy of the final nucleus. It is seen that in general there is good agreement between the data at 43 and 30 Mev. One has to take into account the possibility that some peaks may not appear at a given angle because of strong oscillations in cross section as a function of scattering angle. The positions of the peaks in the spectrum appear to be slightly different. It is doubtful whether any significance can be attached to the discrepancy. *Note added in proof.* Dr. Wall has informed us that corrections in the energy

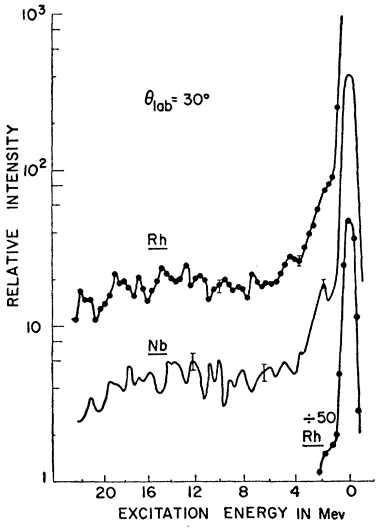

FIG. 6. The inelastic α-particle spectra from Rh and Nb at 30° in the laboratory system. The abscissa is the excitation energy of the final nucleus. The points together with representative errors are shown for Rh. For Nb the curve has been drawn through the experimental points.

scale made after publication of reference 14 have lowered the energies by amounts varying from 0.3 to 1 Mev.

The spectra for Rh and Nb are shown in Fig. 6 and for Au and Ta in Fig. 7. In Rh at an excitation of 2.5 Mev there is a peak which was clearly resolved by inserting additional absorbers. A similar group was observed in Ag. In Nb there is a significant group at 3 Mev. In Au and Ta, any gross structure which might be present could not be resolved. It is to be noted, however, that the qualitative similarity of the energy spectra indicates a similar contribution in both cases from α particles leaving the target nuclei in excited states between 1 and 3 Mev.

In the case of the 2.5-Mev levels of Ag and Rh, angular distributions were obtained. The angular distri-

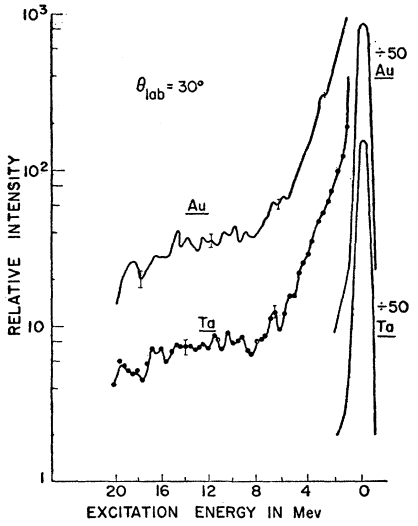

FIG. 7. The inelastic α-particle spectra from Ta and Au at 30° in the laboratory system. The abscissa is the excitation energy of the final nucleus. The points together with representative errors are shown for Ta. For Au the curve has been drawn through the experimental points.

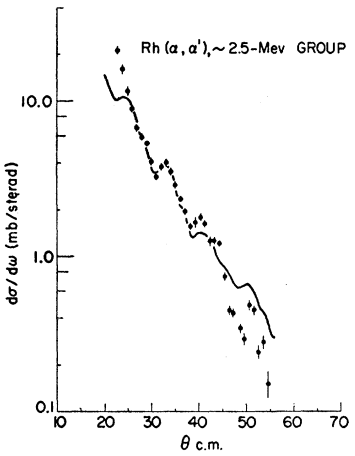

FIG. 8. The differential cross section for the 2.5-Mev group from Rh. The curve is $(Q^2+K^2)^{-2}[j_1^2(QR)+j_2^2(QR)]$, where $R=8.3$ f.

bution for the Rh group is shown in Fig. 8 and the results for Ag are similar. Some attempts were made to fit the data with analytical expressions. The curve drawn through the points was obtained from $(Q^2+K^2)^{-2}\times[j_1^2(QR)+j_2^2(QR)]$, where $\mathbf{Q}$ is the momentum transfer, R is the interaction radius, j_1 and j_2 are spherical Bessel functions, and $(Q^2+K^2)^{-2}$ is a form factor for which K was obtained empirically. Butler[25] has obtained an expression for the differential cross section in which the primary angular dependence is contained in a function $W_l(QR)$ which will be discussed below. For a choice of $l=1$ and $R=8.3$ fermis, $(Q^2+K^2)^{-2}W_l^2(QR)$ gives maxima at approximately the same angles as in the sum of spherical Bessel functions, but the function is zero at the minima.

For Zn, data were obtained at 1° intervals from 10° to about 55° for the 2.8-Mev group and from 30° to 55° for the 1.04-Mev level. The data for the 2.8-Mev group are shown in Fig. 9, together with the curve

$$[(Q^2+K^2)^{-1}j_l(QR)]^2, \quad l=2. \tag{1}$$

The value of K is slightly less than the one which would be obtained from the theoretical expression by inserting a reasonable value of the binding energy B of the struck nucleon, $B=\hbar^2K_i^2/2m_n$; $K=K_i+K_f$; and R was chosen to be 6.85 fermis.

A very similar fit may be obtained by using $l=3$ with $R=7.6$ fermis, but the first peak occurs at 13°, a somewhat larger angle than for $l=2$.

One would like to compare the data with the Butler theory of direct reactions.[25] In this theory the angular dependence is given by

$$[(Q^2+K^2)^{-1}W_l(QR)]^2, \tag{2}$$

where K is determined from the binding energy of the struck nucleon, R is the interaction radius, $\mathbf{Q}$ is the momentum transfer vector, and $W_l(QR)$ denotes a Wronskian which may be defined as

$$W_l(QR)=\left[j_l(Qr)\frac{\partial}{\partial r}h_l(iKr)-h_l(iKr)\frac{\partial}{\partial r}j_l(Qr)\right]_R$$
$$=C[j_l(QR)-\gamma_lQj_{l+1}(QR)], \tag{3}$$

where $h_l(iKr)$ is the spherical Hankel function of order l, C and γ_l are appropriate functions of l and KR, and the expression is evaluated at $r=R$.

For small values of $\mathbf{Q}$, $W_l(QR)$ oscillates essentially as $j_l(QR)$ and for large values of $\mathbf{Q}$ as $j_{l+1}(QR)$. In the present case, the second term becomes dominant at about 30°. The results of Eq. (2) for $R=7.15$ fermis and $l=3$ is shown in curve (a) of Fig. 10. It is seen that the general oscillation pattern of the data is reproduced, but the intensities at the peaks of the oscillations do not vary satisfactorily with angle. Attempts to fit the data with $l=2$ were unsuccessful for all radii. Butler has pointed out that his derivation implicitly assumes that the scattering of the incident nucleons is isotropic in the center-of-mass system. To be more specific, Butler's theory for inelastic scattering due to direct reactions[25] includes the assumption that the primary two-body interaction between the incident particle and

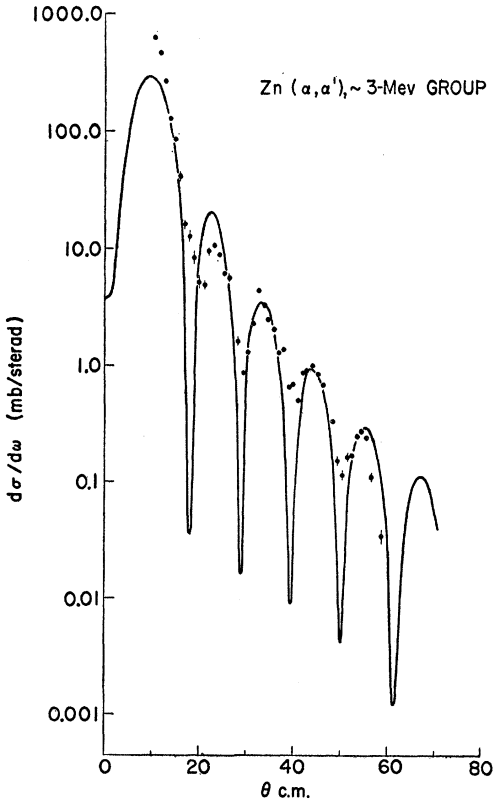

FIG. 9. The differential cross sections of the 2.8-Mev group in Zn. The curve is given by $[(Q^2+K^2)^{-1}j_2(QR)]^2$, where $R=6.85$ f. The errors are smaller than the points, unless shown.

[25] S. T. Butler, Phys. Rev. **106**, 272 (1957).

the target nucleus consists of a contact interaction between the incident particle and a bound nucleon near the surface of the nucleus. This interaction is represented by $V(\mathbf{r}_\alpha-\mathbf{r}_n)$ and is set equal to $V_0\delta(\mathbf{r}_\alpha-\mathbf{r}_n)$ in Butler's treatment. This choice of potential implies that the primary interaction is isotropic. For the interaction of α particles and nucleons, this is not a valid assumption since the experimental data for n-α scattering with 14-Mev neutrons[26] and p-α scattering with 10-Mev protons[27] are clearly not isotropic.

The simple Butler theory using undistorted plane waves may easily be modified to include the effects of anisotropy in the alpha-nucleon interaction. As will be shown below, the simple Butler theory may be corrected to take account of this effect by multiplying it by the differential cross section for α-p scattering at the angle θ, where θ is the scattering angle in the center-of-mass system either for the α particle and nucleus or for the α particle and the nucleon.

The formula for inelastic scattering of an α particle by a nucleus is given by Butler as

$$\sigma(\mathbf{k}_\alpha,\mathbf{k}_\alpha')=\frac{M_\alpha^2}{(2\pi\hbar^2)^2}\frac{k_\alpha'}{k_\alpha}\sum_{\text{Av}}|I(\mathbf{k}_\alpha,\mathbf{k}_\alpha')|^2, \tag{4}$$

where M_α is the mass of the α particle and $\mathbf{k}_\alpha$ and $\mathbf{k}_\alpha'$ are the incident and outgoing wave vectors for the α particles, $|\mathbf{k}_\alpha|=(2M_\alpha E_\alpha/\hbar^2)^{\frac{1}{2}}$. Also

$$I(\mathbf{k}_\alpha,\mathbf{k}_\alpha')=\int d\xi d\mathbf{r}_n d\mathbf{r}_\alpha\, v_0(\xi,\mathbf{r}_n)v_t^*(\xi,\mathbf{r}_n)V_{\alpha,n}(\mathbf{r}_\alpha-\mathbf{r}_n)\times\psi_\alpha(\mathbf{k}_\alpha,\mathbf{r}_\alpha)\psi_{\alpha,t}^*(\mathbf{k}_\alpha',\mathbf{r}_\alpha), \tag{5}$$

where v_0 and v_t are the wave functions describing the target nucleus in the initial and final states, respectively, ψ_α and $\psi_{\alpha,t}$ are the wave functions that describe the alpha particle before and after the scattering, $V_{\alpha,n}(\mathbf{r}_\alpha-\mathbf{r}_n)$ is the primary two-particle potential between the α particle and a nucleon in the nucleus, $\mathbf{r}_\alpha$ and $\mathbf{r}_n$ are the position vectors of the α particle and the bound nucleon in the nucleus, and ξ represents all the variables for all the other nucleons in the target except the one indicated by $\mathbf{r}_n$.

When the plane-wave approximation is used, ψ_α and $\psi_{\alpha,t}^*$ may be written as

$$\begin{aligned}&\psi_\alpha(\mathbf{k}_\alpha,\mathbf{r}_\alpha)\sim\exp[i\mathbf{k}_\alpha\cdot(\mathbf{r}_\alpha-\mathbf{r}_n)]\exp(i\mathbf{k}_\alpha\cdot\mathbf{r}_n),\\&\psi_{\alpha,t}^*(\mathbf{k}_\alpha',\mathbf{r}_\alpha)\sim\exp[-i\mathbf{k}_\alpha'\cdot(\mathbf{r}_\alpha-\mathbf{r}_n)]\exp(-i\mathbf{k}_\alpha'\cdot\mathbf{r}_n).\end{aligned} \tag{6}$$

On changing to the variables $\mathbf{x}=\mathbf{r}_\alpha-\mathbf{r}_n$ and $\mathbf{Q}\equiv\mathbf{k}_\alpha-\mathbf{k}_\alpha'$ and substituting in the formula above, one has

$$I(\mathbf{k}_\alpha,\mathbf{k}_\alpha')\sim\int d\mathbf{x}\, V_{\alpha,n}(\mathbf{x})\exp(i\mathbf{Q}\cdot\mathbf{x})\int d\xi d\mathbf{r}\times v_0(\xi,\mathbf{r}_n)v_t^*(\xi,\mathbf{r}_n)\exp(i\mathbf{Q}\cdot\mathbf{r}_n). \tag{7}$$

[26] J. D. Seagrave, Phys. Rev. **92**, 1222 (1953).
[27] T. M. Putnam, Phys. Rev. **87**, 932 (1950).

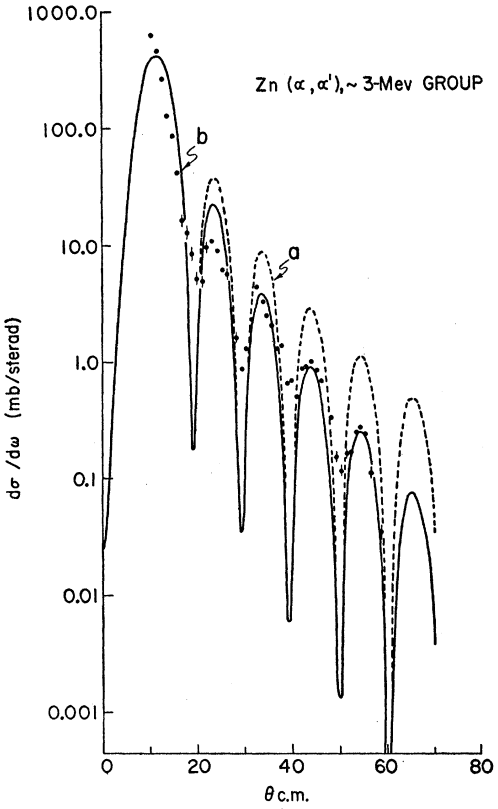

FIG. 10. The differential cross section of the 2.8-Mev group in Zn. (a) $[(Q^2+K^2)^{-1}W_3(QR)]^2$ where $R=7.15$ f. (b) $[(Q^2+K^2)^{-1}W_3(QR)]^2(d\sigma/d\omega)_{\alpha,p}$, where $R=7.15$ f and $(d\sigma/d\omega)_{\alpha,p}$ is the differential cross section for the scattering of 43-Mev α particles by hydrogen. The errors are smaller than the points, unless shown.

This formula is equivalent to the Butler approximation, Eq. (39) of reference 25, except that V_0 has been replaced by $\int d\mathbf{x}\, V_{\alpha,n}(\mathbf{x})\exp(i\mathbf{Q}\cdot\mathbf{x})$. This last term is just the Born approximation to the scattering amplitude for alpha-nucleon scattering. In particular if $|\mathbf{k}_\alpha|\cong|\mathbf{k}_\alpha'|$, this is just the Born approximation to the scattering amplitude for *elastic* alpha-nucleon scattering. This immediately leads to

$$\sigma(\mathbf{k}_\alpha,\mathbf{k}_\alpha')\sim\sigma_{\text{elastic}}(\mathbf{k}_\alpha,\mathbf{k}_\alpha)\sigma_{\text{Butler}}(\mathbf{k}_\alpha,\mathbf{k}_\alpha'), \tag{8}$$

where $\sigma_{\text{elastic}}(\mathbf{k}_\alpha,\mathbf{k}_\alpha)$ is the elastic scattering cross section for α particles on nucleons, either in the Born application or better still obtained from the actual experimental results, and $\sigma_{\text{Butler}}(\mathbf{k}_\alpha,\mathbf{k}_\alpha')$ is the Butler expression for the inelastic scattering of α particles by nuclei.

When the correction is applied to Eq. (2) on the basis of the p-α data of Putnam,[27] then curve b in Fig. 10 is obtained. Satisfactory agreement is also obtained when the correction is applied to Eq. (1) if a slightly larger value of K is used, i.e., if the struck nucleon is considered to be slightly more tightly bound. The curve for this case is the same as the one in Fig. 9.

From the preceding discussion it follows that it is

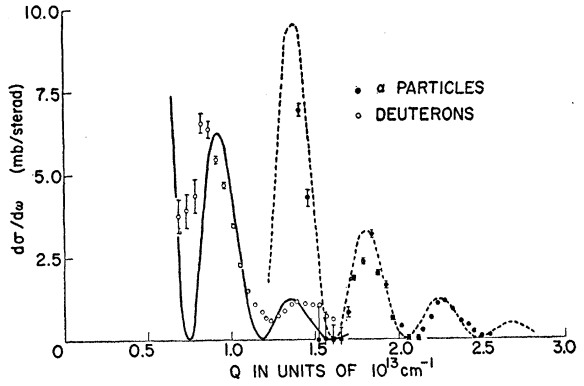

FIG. 11. The differential cross section for the scattering of 21.6-Mev deuterons and 43-Mev α particles from the 1.04-Mev level of Zn. The abscissa is the momentum transfer. The solid curve is given by $[(Q^2+K^2)^{-1}W_2(QR)]^2(d\sigma/d\omega)_{d,n}$. The dashed curve is given by $[(Q^2+K^2)^{-1}W_2(QR)]^2(d\sigma/d\omega)_{\alpha,p}$. R was chosen to be 7.1 f. The errors are smaller than the points, unless shown.

not possible to infer the spins and parities of the states represented in the 2.8-Mev group, since it is possible to fit the data with functions corresponding to a change in angular momentum of either 2 or 3 units. A transition in which the angular momentum change is known to be 2 units is that involving the excitation of the 1-Mev level in the zinc isotopes. The data from inelastic scattering of 43-Mev alpha particles and 21.6-Mev deuterons are shown in Fig. 11.

In order to make the comparison with theory more direct, both angular distributions are plotted in terms of the momentum transfer $\mathbf{Q}$ rather than in terms of the center-of-mass scattering angle. The theoretical curves are the Butler angular distribution formula $[(Q^2+K^2)^{-1}W_2(QR)]^2$ modified by (a) the d-n elastic scattering data[28] when applied to the inelastic deuteron results or (b) the α-p elastic scattering[27] when applied to the inelastic α-particle results. This results in the formula

$$\frac{d\sigma}{d\omega}(\mathbf{Q})\sim\frac{d\sigma}{d\omega}(\mathbf{Q})_{\text{elastic}}[(Q^2+K^2)^{-1}W_2(QR)]^2, \quad (9)$$

where $\mathbf{Q}\equiv\mathbf{k}_i-\mathbf{k}_f$ for both the elastic scattering and the inelastic scattering. The choice of l value was restricted to $l=2$ because of the known change of angular momentum in this reaction, and the radius R was chosen to be 7.1 fermis. The theory is very sensitive to changes in R and less than a 2% decrease in R would move the theoretical curves into almost exact agreement with the inelastic alpha data. The curves indicate the theoretical fits to the data when the Butler formalism is modified by the correction previously discussed. It is not possible to reproduce the experimentally determined variation in peak intensities if spherical Bessel functions are used, since too strong a falloff is predicted even without the correction. It is therefore seen that in order to fit the 1-Mev data, it is necessary to use the modified Butler formalism, with $R=7.1$ fermis. A consistent picture of the inelastic scattering of α particles is then obtained if one considers the scattering as being described by the modified Butler formalism with $R=7.1$ fermis and $l=2$ for the 1-Mev states and $R=7.1$ fermis and $l=3$ for the 2.8-Mev group.

[28] J. D. Seagrave, Phys. Rev. **97**, 757 (1955).

ACKNOWLEDGMENTS

We wish to acknowledge several helpful discussions with Dr. S. T. Butler and Dr. M. Hamermesh. We are indebted to P. H. Liebenauer and J. Garner for the analysis of part of the data and to W. J. O'Neill and E. Sundahl for technical assistance. The cooperation of W. Ramler and the cyclotron group is gratefully acknowledged.